

Central Lancashire Online Knowledge (CLoK)

Title	Analytic and In Silico Methods to Understand the Interactions between
	Dinotefuran and Haemoglobin
Type	Article
URL	https://clok.uclan.ac.uk/id/eprint/52452/
DOI	https://doi.org/10.1002/cbdv.202400495
Date	2024
Citation	Yadav, Sandeep, Sewariya, Shubham, Singh, Prashant, Chandra, Ramesh, Jain, Pallavi and Kumari, Kamlesh (2024) Analytic and In Silico Methods to Understand the Interactions between Dinotefuran and Haemoglobin. Chemistry & Biodiversity, 21 (8). ISSN 1612-1880
Creators	Yadav, Sandeep, Sewariya, Shubham, Singh, Prashant, Chandra, Ramesh, Jain, Pallavi and Kumari, Kamlesh

It is advisable to refer to the publisher's version if you intend to cite from the work. https://doi.org/10.1002/cbdv.202400495

For information about Research at UCLan please go to http://www.uclan.ac.uk/research/

All outputs in CLoK are protected by Intellectual Property Rights law, including Copyright law. Copyright, IPR and Moral Rights for the works on this site are retained by the individual authors and/or other copyright owners. Terms and conditions for use of this material are defined in the http://clok.uclan.ac.uk/policies/





Accepted Article

Title: Analytic and In Silico Methods to Understand the Interactions between Dinotefuran and Haemoglobin

Authors: Sandeep Yadav, Shubham Sewariya, PRASHANT SINGH, Ramesh Chandra, Pallavi Jain, and Kamlesh Kumari

This manuscript has been accepted after peer review and appears as an Accepted Article online prior to editing, proofing, and formal publication of the final Version of Record (VoR). The VoR will be published online in Early View as soon as possible and may be different to this Accepted Article as a result of editing. Readers should obtain the VoR from the journal website shown below when it is published to ensure accuracy of information. The authors are responsible for the content of this Accepted Article.

To be cited as: Chem. Biodiversity 2024, e202400495

Link to VoR: https://doi.org/10.1002/cbdv.202400495

WILEY-VHCA

Analytic and *In Silico* Methods to Understand the Interactions between Dinotefuran and Haemoglobin

Sandeep Yadav, \$\,^{\\$,1,2}\$ Shubham Sewariya, \$\,^{\\$,3,4}\$ Prashant Singh \$^{1,2,*}\$ Ramesh Chandra, \$^3\$ Pallavi Jain, \$^2\$ Kamlesh Kumari \$^5,*

¹Department of Chemistry, Atma Ram Sanatan Dharma College, University of Delhi, New Delhi, India;

²Department of Chemistry, SRM Institute of Science & Technology, Delhi-NCR Campus, Modinagar, Ghaziabad, India;

³Department of Chemistry, University of Delhi, Delhi, India;

⁴School of Pharmacy and Biomedical Sciences, University of Central Lancashire, Preston, United Kingdom;

⁵Department of Zoology, University of Delhi, Delhi, India

\$ equal authorship

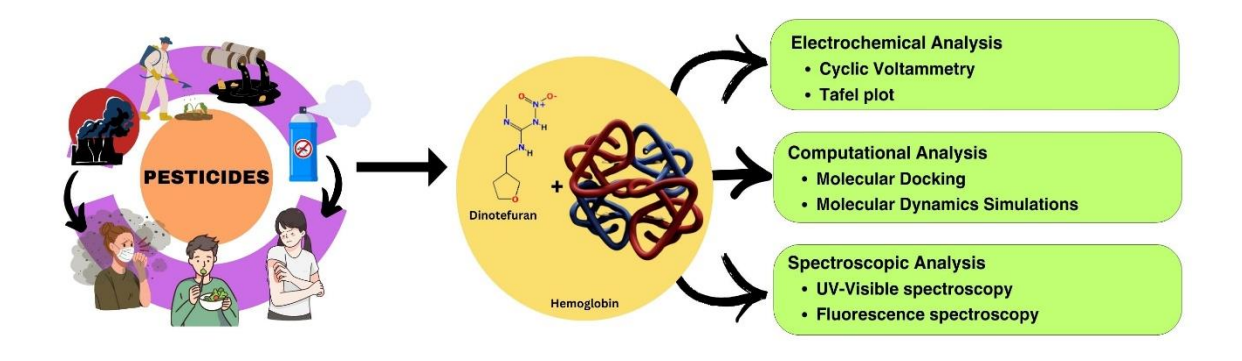
* Corresponding author

Email: psingh@arsd.du.ac.in and kkumari@zoology.du.ac.in

Abstract

This work lies in the growing concern over the potential impacts of pesticides on human health and the environment. Pesticides are extensively used to protect crops and control pests, but their interaction with essential biomolecules like haemoglobin (Hb) remains poorly understood. Spectrofluorometric, electrochemical, and *in silico* investigations have been chosen as potential methods to delve into this issue, as they offer valuable insights into the molecular-level interactions between pesticides and haemoglobin. The research aims to address the gaps in knowledge and contribute to developing safer and more sustainable pesticide practices. The interaction was studied by spectroscopic techniques (UV-Visible & Fluorescence), *in silico* studies (molecular docking & molecular dynamics simulations) and electrochemical techniques (cyclic voltammetry and tafel). The studies showed effective binding of dinotefuran with the Hb and will cause toxicity to human. The formation of a stable molecular complex between ofloxacin and Haemoglobin was shown via molecular docking and the binding energy was found to -5.37 kcal/mol. Further, molecular dynamics simulations provide an insight for the stability of the complex (Hb-dinotefuran) for a span of 250 ns with a binding free energy of -53.627 kJ/mol. Further, cyclic voltammetry and tafel studies for the interaction of dinotefuran with Hb effectively.

Keywords: Pesticides; Haemoglobin; Spectroscopy; Molecular Dynamics Simulations; Electrochemical Studies



1. Introduction

Pesticides and agrochemicals have played critical roles in contemporary agriculture, considerably increasing crop yields and food production during the last century. With the world human population continually expanding, the need for improved food production has become ever more pressing. However, this requirement is exacerbated by conflicts and the effects of climate change, which intensify food shortages in diverse places, demanding more food production efforts [1]. Despite its advantages, pesticide usage has raised worries about the environmental and health consequences [2]. Agrochemical residues have been found to diffuse throughout the environment, resulting in significant pollution of terrestrial ecosystems and human food supplies. Furthermore, pesticide contamination has harmed aquatic systems, especially tropical coastal ecosystems, threatening aquatic food supplies, fisheries, and aquaculture [3]. Pesticides are a broad group of chemical substances that have been purposefully engineered to exert desired modes of action and successfully target certain species^[4]. Strict control and appropriate pesticide application are required to guarantee sustainable farming practises and prevent negative consequences [5]. To ensure agricultural systems' long-term survival, integrated pest management solutions integrating biological controls, crop rotation, and environmentally friendly practises should be advocated [6]. While pesticides have played an important role in satisfying a growing population's rising food demand, their use must be controlled carefully to balance agricultural production and environmental preservation, while prioritizing human health and food security. Groups at high risk of direct pesticide exposure comprise workers engaged in various stages of pesticide handling, including formulators, sprayers, mixers, loaders, and agricultural farm workers [7]. Manufacturing and formulation procedures are more dangerous since they involve interaction with hazardous chemicals and conditions. Workers are exposed to pesticides directly via skin contact and inhalation of airborne toxins [1]. Workers in industrial environments face additional hazards because they are exposed to various harmful compounds, including insecticides, raw materials, toxic solvents, and inert carriers. Indirect pesticide exposure occurs when people come into touch with polluted soil, air, water, or food, resulting in a wide range of health impacts [8]. Pesticide exposure can occur directly through occupational, agricultural, and residential use, as well as indirectly through food sources [9]. The general population may also encounter pesticides in nonagricultural settings, such as golf courses and areas near major roads. Human exposure to pesticides occurs through ingestion of contaminated food, inhalation of pesticide-laden air, dermal

contact, and interaction with contaminated water, soil, flora, and fauna [10]. Once inside the body, pesticides disperse through the bloodstream and can be excreted through urine, skin, and exhaled air. Pesticides enter the human body primarily by skin exposure, oral exposure, ocular exposure, and respiratory exposure (inhalation) [11][12]. Pesticide toxicity varies based on the route of exposure, whether cutaneous, oral, or respiratory. In addition to the inherent toxicity of the individual chemical implicated, the danger of pesticide contamination often increases with larger concentrations and during key periods of exposure [13]. Implementing adequate safety measures, laws, and protective equipment is critical to reducing the dangers of pesticide exposure and protecting human health in pesticide-related jobs and surroundings [14].

Dinotefuran is a furanicotinyl insecticide from the third generation of neonicotinoids that works as an agonist of insect nicotinic acetylcholine receptors, resulting in wide insecticidal action [15]. Because of its low toxicity, excellent efficiency, and broad-spectrum efficacy against a variety of dangerous pests, it is frequently employed in agriculture. It is used to manage the dangerous pest Empoasca, pirisuga, Matumura, in tea farming in China [16][17][18]. However, the presence of dinotefuran and its metabolites in the final product raises food safety issues as well as possible human health hazards. Despite its benefits, dinotefuran is very harmful to pollinators and aquatic species [19]. Because of the dangers of dinotefuran, quantitative detection is crucial. Dinotefuran, often known as "furan nicotine," outperforms other nicotine pesticides in pest control due to its unusual chemical composition that lacks halogenated components [20]. It inhibits acetylcholinesterase in pests, interrupting neurotransmission and exhibiting broad insecticidal efficacy against a variety of pest species [21]. However, environmental conditions such as hydrolysis and photolysis might impair its potency, resulting in decreased availability [20]. Furthermore, utilising dinotefuran alone may contribute to pesticide resistance, emphasising the significance of combining synergistic pest management techniques to eliminate pests while minimizing resistance development effectively [22].

Haemoglobin is a crucial protein necessary for transporting oxygen in vertebrates, including humans. It is primarily found in red blood cells and plays a vital role in capturing oxygen in the lungs and distributing it to different tissues throughout the body. This process is essential for supporting critical metabolic functions that depend on oxygen^[23]. Researchers investigated Haemoglobin adducts of aromatic amines released from pesticides. The study's findings suggest that arylamine-Haemoglobin adducts could potentially serve as a valuable method for measuring

the bioavailability of potentially hazardous pesticide components [24]. The molecular docking analysis of 10 pesticides with five targeted proteins reveals that the cytochrome P450 protein has a maximum binding energy of -45.21 relative units to the pesticide phosmet ^[25]. Buss et. al. studied the interaction of pesticides and insecticides with p-glycoprotein [26]. Arif et. al. examined the interaction between human Haemoglobin and bio allethrin using both in silico and biophysical approaches. Molecular docking and Discovery Studio visualisation were employed to understand the molecular interaction better. The results confirmed the formation of a stable Hb-bioallethrin complex with a binding energy of -7.3 kcal/mol [27]. This study farmers who were intermittently exposed to organophosphorus and carbamate pesticides for more than five years were analyzed. The findings indicate that approximately 85% of the participants exposed to pesticides for this duration exhibited signs of pesticide toxicity. Among the participants who tested positive for pesticide presence, the levels of Paraoxanase I were lower than those found in the control group of normal participants [28]. Emadi et al. study that Cartap causes a reduction in standard functionality and has a negative impact on both the oxygen affinity and transport capacity of Haemoglobin (Hb). Additionally, the thermodynamic reveals that the presence of Cartap leads to a decrease in the stability of Hb [29]. Tetraethyl pyrophosphate (TEPP) exhibits to dissolve REC and permeate RBCs. Moreover, it can interact with the internal heme prosthetic group and induce heme degradation upon interaction with Hb [30].

In this work, authors have investigated pesticide interaction (Dinotefuran) with Haemoglobin using UV-Visible spectroscopy and fluorometry. Further, authors have explored molecular docking and molecular dynamics simulations, followed by electrochemical studies (cyclic voltammetry and tafel techniques).

2 Methods

2.1 Spectroscopic techniques

2.1.1 UV-Visible spectroscopy

UV-Visible absorption spectroscopy is a suitable method to comprehend the interactions between proteins and ligands as well as the resulting conformational changes in the protein structure. The UV-Visible spectra was recorded at room temperature using Thermo-Scientific Evolution 300 UV-Visible spectrophotometer to gain an insight into the interaction of dinotefuran with human Haemoglobin. First, the spectrum of pure Haemoglobin was recorded at different

concentrations over a range of wavelength from 200 nm to 600 nm. Once, an appropriate concentration corresponding to apt absorbance was found, the respective solution of Haemoglobin in appropriate PBS buffer was held constant and titrated with varying concentrations of dinotefuran at a pH of 7.4 $^{[31,32]}$. We recorded the absorbance at an optimized constant Hb concentration of 2.5 μ M and then upon gradually adding the pesticide from 0 to 100 μ M. The baseline in the experiment was set using a reference solution of 1X PBS (10 mM).

2.1.2 Fluorescence spectroscopy

Fluorescence spectroscopy is a well-established method for examining how proteins interact with ligands, determining how they bind, and calculate the associated biophysical parameters. Steady state fluorescence spectroscopy was performed using Hitachi F-7000 Fluorescence Spectrophotometer. The experiments were performed at λ_{ex} of 280 nm and the corresponding emission spectra was in the range of 300 to 600 nm, slit width was fixed at 5 nm with a scan rate of 2400 nm/min. Different concentration of Haemoglobin have been taken to optimize the concentration at which the steady state fluorescence to be performed. Then the concentration of Haemoglobin was kept constant at 2.5 μ M while treated with gradually increasing concentrations of dinotefuran from 0 to 70 μ M. The spectra for each titration was recorded at 310 K and at a physiological pH of 7.4 [31]. Furthermore, during fluorescence experiments, we need to account for self-quenching combined with the inner filter effect in typical fluorophores (like Hb) only when the concentrations is greater than 10 μ M and the path length is 1 cm. Herein, we are using an optimized 2.5 μ M concentration of Hb and do not need to focus on self-quenching of the fluorophore [33].

The spectra recorded at three different temperatures was used to calculate the associated parameters (using Stern Volmer equation (1) and modified Stern Volmer equation) to investigate the efficacy of the interaction between Haemoglobin and the pesticide (dinotefuran) under screening.

$$\frac{F_o}{F} = I + K_{sv}[Q] = K_q \tau_o[Q] \tag{1}$$

Herein, K_{sv} will be equal to the slope of the straight line. Once the K_{sv} will be computed, K_q , the quenching rate constant of the interaction will be deciphered by using the already reported τ_0 value for Haemoglobin^[34].

The binding constant (K_b) will be calculated by modified Stern Volmer equation (2):

$$log\left(\frac{F_o - F}{F}\right) = logK_b + nlog[Q]$$
 (2)

Wherein F_0 and F are the emission intensity of Haemoglobin in absence/ presence of dinotefuran, n is the no. of binding sites and [Q] represents concentration of dinotefuran.

2.2 In Silico Study

Structures of pesticide was made and optimized by using ChemDraw Professional (Figure 1) [35]. Molecular mechanics 2 was used to optimize the geometry of Dinotefuran, it aims to minimized the energy of the structure by changing the conformation and position of atoms.

Figure 1 Structure of dinotefuran

2.2.1 Molecular docking

To understand the interaction of dinotefuran with different amino acid of Haemoglobin, molecular docking was performed by AutoDock^[36].

2.2.2 Molecular dynamics (MD) simulations To understand the behaviour of dinotefuran in water and their interaction with Hb was investigated by MD simulations using Gromacs ^[37].

Preparation before performing MD simulations Pesticides and different proteins including serum proteins, heme proteins etc will be prepared by chimera 1.8. Appropriate force field on chemical entities will be applied as well as the solvation model will be used to account for the influence of the surroundings.

Equilibration The system will be equilibrated to get a stable configuration and thermal equilibrium. Further, MD simulations will be performed at suitable temperature and pressure.

Production of MD simulation Equilibrated system will be subjected to production MD simulations. Simulations will be run for an extended duration of time to ensure that statistically meaningful data is collected for further analysis. Various parameters like structural fluctuations, intermolecular interactions, and diffusion coefficients will be monitored.

Analysis The trajectories (radial distribution functions, identification of hydrogen bonding patterns, and determination of interaction energies, root mean square deviation, root mean square fluctuation) obtained from the MD simulations will undergo thorough analysis. Free energy will be calculated to understand the system's stability and energetics comprehensively.

2.3 Electrochemical studies:

Electrochemical studies represent a robust suite of analytical methods employed to explore the behavior of chemical entities at the interfaces between electrodes and electrolytes. These methodologies rely on applying electrical potential to induce and quantify redox reactions, adsorption processes, and charge transfer phenomena. Given their distinctive merits, electrochemical studies offer a superior approach for investigating the interactions between water-soluble pesticides and Haemoglobin (Hb). One of the foremost advantages lies in their high sensitivity and selectivity, enabling the precise detection of even subtle alterations in the electrochemical behavior of the involved species, even when present in low concentrations. Moreover, these electrochemical techniques facilitate real-time analysis, enabling the continuous monitoring of dynamic changes in electrochemical responses [38].

- **2.3.1** Cyclic voltammetry provides valuable information about the redox behavior of species in a solution. It involves applying a linear potential scan between two limits while recording the resulting current response. For pesticide-Hb interactions, CV can help identify redox reactions related to both the pesticides and Hb, thus revealing any changes in their electrochemical behavior upon interaction [39].
- **2.3.2 Tafel plot** analysis entails measuring polarization curves while varying the applied potential at different scan rates. Through investigation of reaction kinetics, researchers can gain insights into the nature and extent of interactions between pesticides and Hb. This information is essential for evaluating the potential impact of pesticides on Hb's oxygen-carrying capacity and overall function^[40].
- 3. Results and Discussion
- 3.1 Spectroscopic studies to understand the binding of pesticide with Hb
- 3.1.1 UV-Visible spectral studies

UV-Visible spectroscopy is widely used to understand the interaction between a protein and ligand and the conformational rearrangements in the protein structure due to possible interactions ^[41]. Reduced activity of Paraoxonase, Glucose 6-phosphate dehydrogenase and Human Hb on addition of a ligand have been reported ^[42–44]. In the 200–500 nm for wavelength, Hb exhibits three distinct absorption peaks at 212 nm (n to π^* transitions) indicates the α -helical structure of Hb; at 274 nm (π to π^* transitions) for aromatic amino acid; and the 406 nm is connected to the Soret band of porphyrin ^[45–51]. With steadily rising dinotefuran concentrations from 0 to 100 μ M, authors find an increase in the absorbance of Hb at 278 nm and a weak shift at 406 nm as shown in **Figure 2**. It is possible to conclude that dinotefuran strongly binds Hb, point to formation of complex (dinotefuran-Hb). Concurrently from the UV-Visible spectrum, we can infer that the pesticide and Hb are forming a stable ground state complex and the nature of quenching is static in nature. In case of collisional encounters and dynamic quenching, there is negligible change in the absorption spectrum^[52].

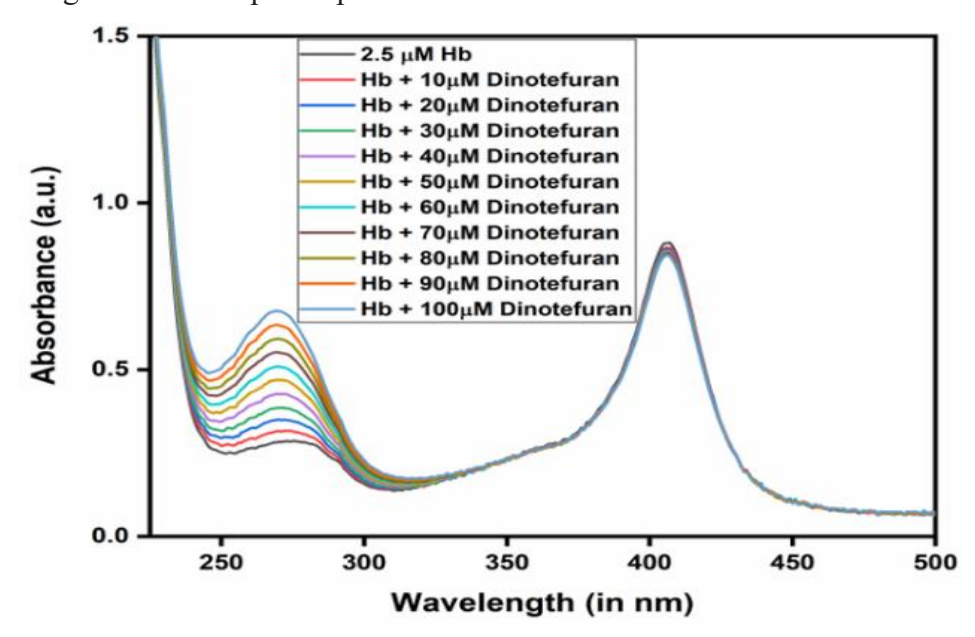


Figure 2: UV-Visible spectra of Hb against varying concentrations of Dinotefuran at 298 K

3.1.2 Fluorescence spectral studies

One of the conventional techniques to understand protein-dinotefuran interactions and proper assessment of the binding mechanism is fluorescence spectroscopy. The intrinsic fluorescence of Haemoglobin is mainly due to β -Trp37 residue present in the tetrameric protein [53,54]. In the absence of any dinotefuran, Hb exhibits a fluorescent emission band at 336 nm upon

exciting at 280 nm; authors have observed a reduction in emission intensity without any shift in wavelength, upon successively increasing amount of dinotefuran from 0 to 70 μ M, as illustrated in **Figure 3**. Our assertion of the interaction between the dinotefuran and Hb might occurs around the β -Trp37 residue as we do not see any wavelength shifts in the spectra. The results derived from absorption spectrum measurements, are reinforced by the fluorescence quenching that occurs when the dinotefuran is introduced in higher amounts.

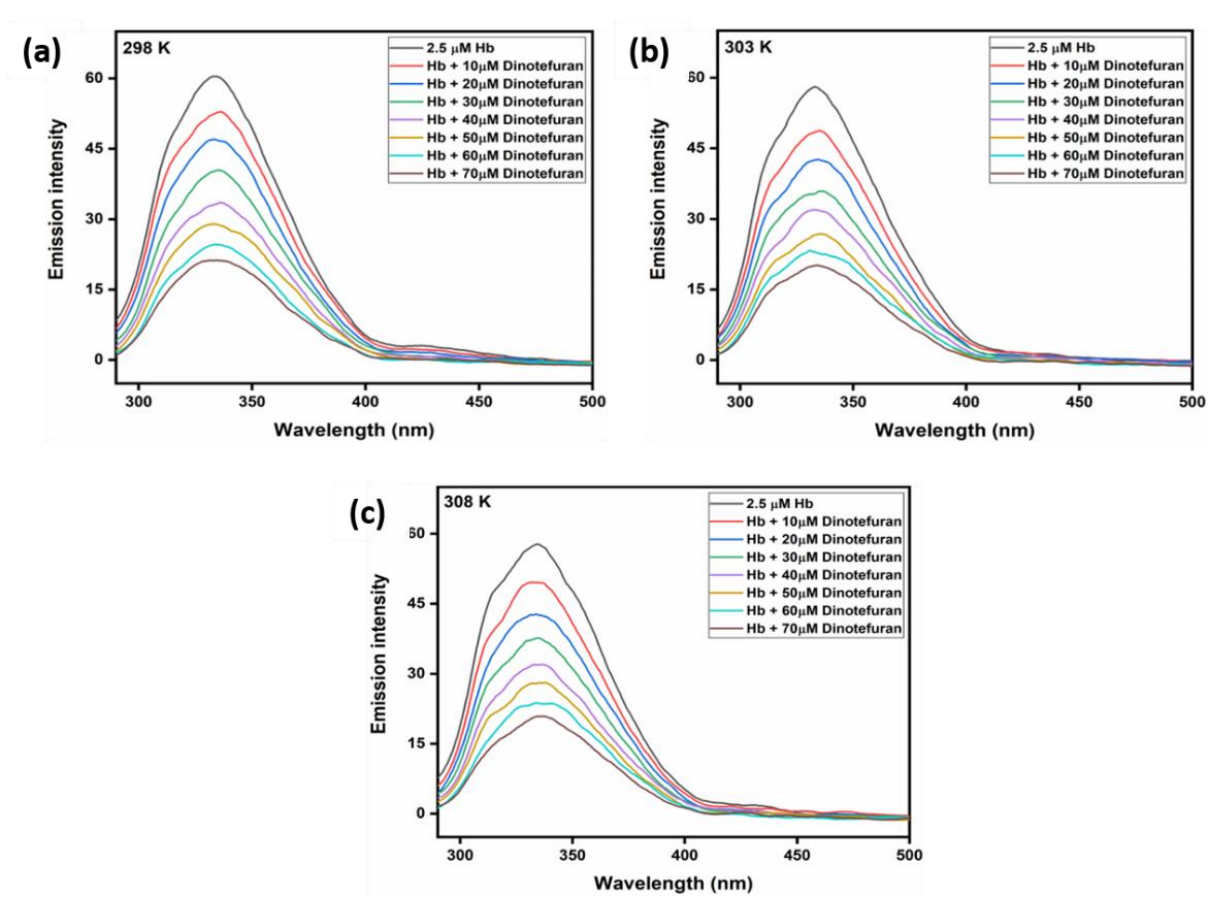


Figure 3: Emission spectra of Hb against changing concentrations (0 to 280 μ M) of dinotefuran at (a) 298 K, (b) 303 K and (c) 308 K

Authors have evaluated the fluorescence spectral data at various temperatures (298, 303 & 308 K) to understand the mechanism of quenching and other parameters (**Figure 3**) [55–57], [57,58], [59]. The plot of F_o/F against [Q] shown in **Figure 4a** was linear for varying the concentration of dinotefuran (0 to 70 μ M) K_q and K_{sv} have been calculated (listed in **Table 1**). Authors observed a linear plot and thus, bimolecular quenching constants is 10^{12} M⁻¹s⁻¹, higher than the maximum scattering collisional quenching constant [60–63] i.e., 2 X 10^{10} M⁻¹s⁻¹. Thus, authors inferred that the

16121880, ja, Downloaded from https://onlinelibrary.wiley.com/doi/10.1002/cbd

Chemistry & Biodiversity 10.1002/cbdv.202400495

quenching is static quenching in nature during dinotefuran-Hb binding. Under the assumption that Hb has independent binding sites, we utilized the modified Stern-Volmer equation and calculated the binding constant as well as number of binding sites in the complex ^[56]. (Figure 4b)

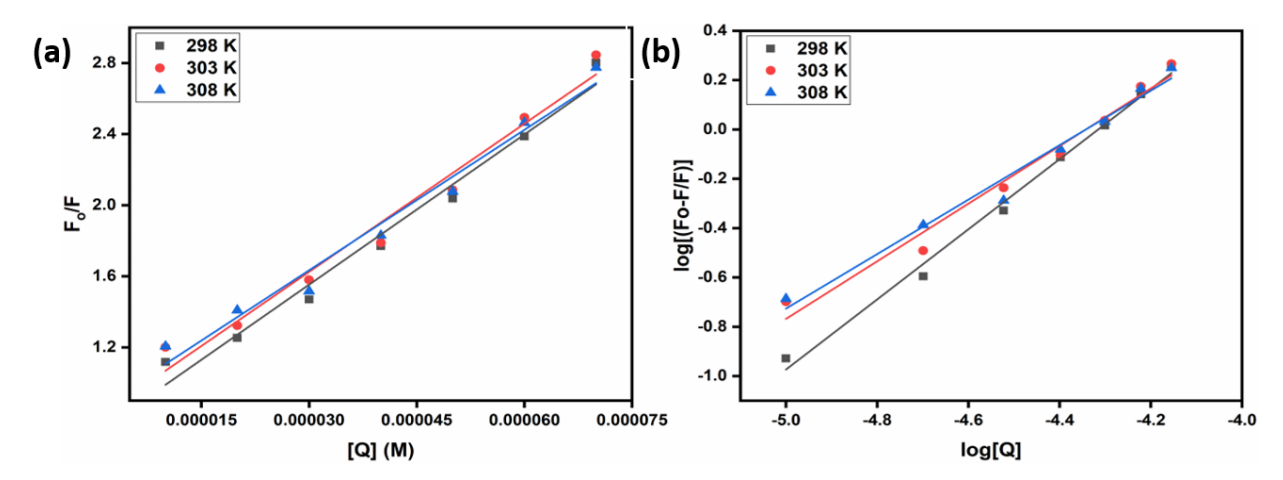


Figure 4: (a) Stern-Volmer plot (b) Modified Stern-Volmer plot; of Hb against varying concentrations of Dinotefuran (0 to $70 \mu M$) at different temperatures

Table 1: Stern Volmer and bimolecular Quenching constants for Dinotefuran-Hb binding at 298 K, 303 K and 308 K

Temperature (K)	Ksv (M ⁻¹) X 10 ⁴	$K_q (M^{-1}s^{-1}) \times 10^{12}$
298	2.817	2.817
303	2.780	2.780
308	2.635	2.635

At 298 K, the binding constant was found to be $1.362 \times 10^6 \text{ M}^{-1}$ (**Table 2**) for dinotefuran-Hb binding. The value of n is nearly one and therefore, the complex formed between the dinotefuran and Hb is formed in a ratio of 1:1. Further, authors determined thermodynamic parameters for the dinotefuran-Hb complex from the Van't Hoff's plot shown in **Figure 5**.

16121880, ja, Downloaded from https://onlii

Chemistry & Biodiversity 10.1002/cbdv.202400495

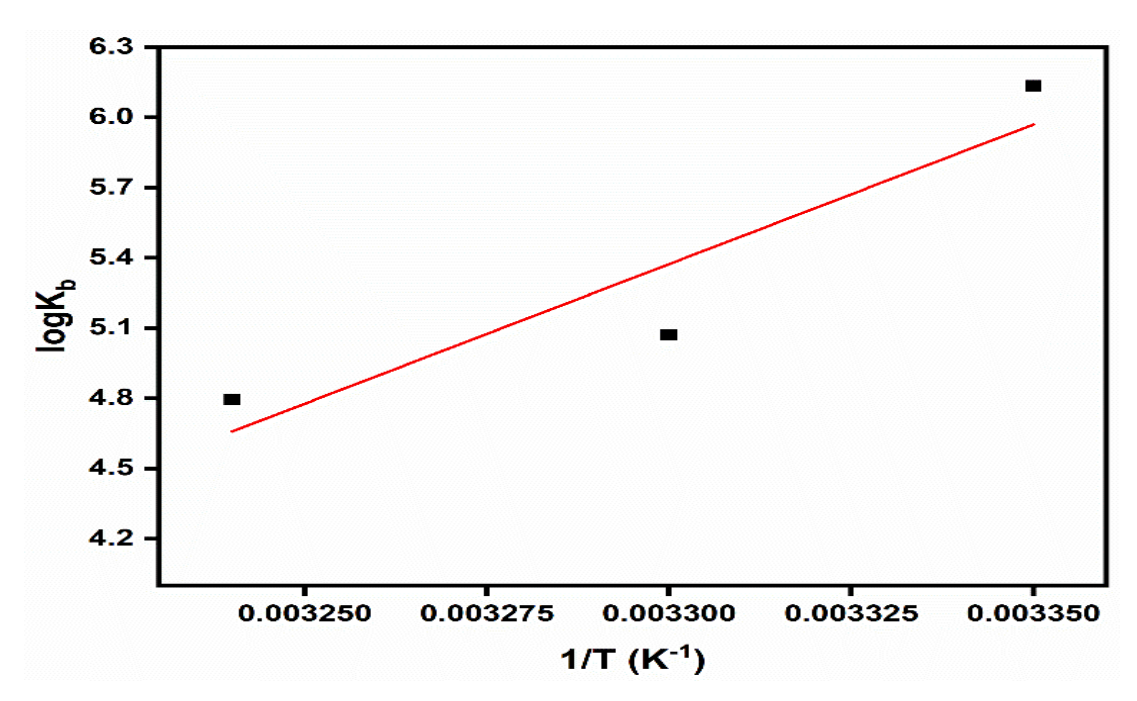


Figure 5: Van't Hoff's plot for Hb-dinotefuran interaction

Table 2: Thermodynamic parameters of Hb-dinotefuran binding	Table 2: 7	Thermodynami	c parameters c	of Hh-dinotefuran	binding
---	------------	--------------	----------------	-------------------	---------

Temperature	K _b (M ⁻¹)	n	ΔG (KJmol ⁻¹)	ΔH (KJmol ⁻¹)	ΔS (Jmol ⁻¹ K ⁻¹)
(Kelvin)					
298	1.362 X 10 ⁶	1.42			
			-34.448	-228.378	-650.769
303	1.177 X 10 ⁵	1.16			
308	62,330	1.10			

3.2 In silico studies to understand the binding of dinotefuran with Hb at molecular level

3.2.1 Molecular docking

The nature of the dinotefuran-Hb interacting forces can be inferred from the magnitude of energy values, i.e., hydrophobic, Van der Waals, hydrogen bonding, and electrostatic interactions [64–67]. The binding energy for the formation of complex was found to be -5.37 kcal/mol. More negative binding energy infers a stable complex of ligand and protein. Hydrophobic interactions were observed between the tetrahydrofuran ring and VAL 93, LEU 101 and PHE 98 with a distance of 5.95 Å, 4.44 Å and 3.65 Å, respectively. Whereas the oxygen atoms of the nitro group formed hydrogen bond with SER 133 and PHE 98 amino acids with a bond length of 3.54 Å and 4.18 Å,

respectively. Figure 6 illustrates the interacting view of Dinotefuran with various aminoacids of Hb at one of the target site.

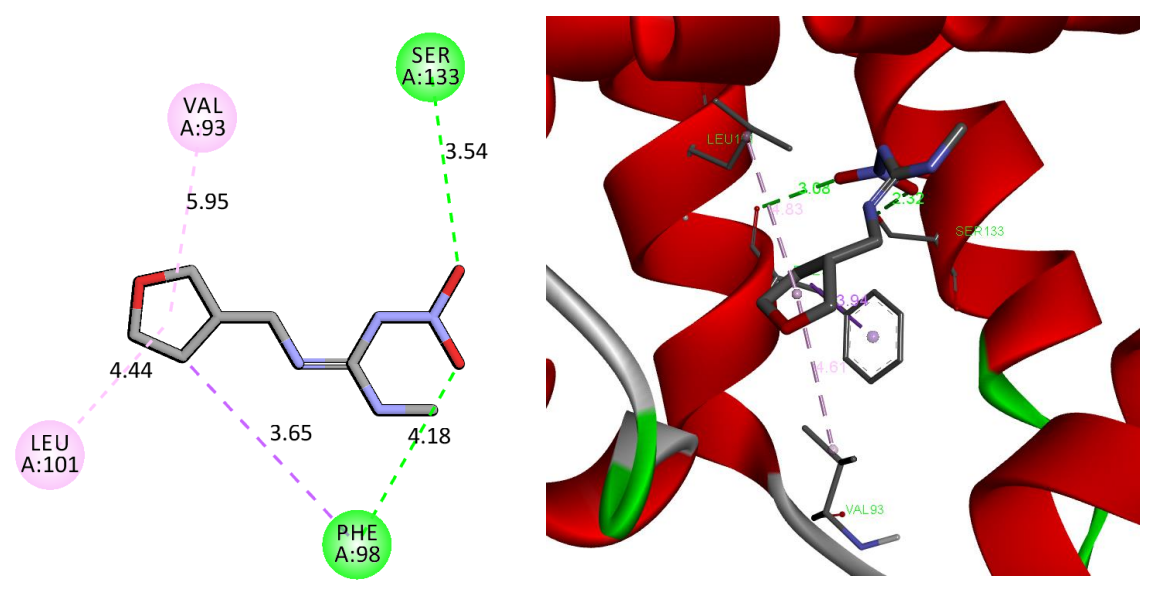
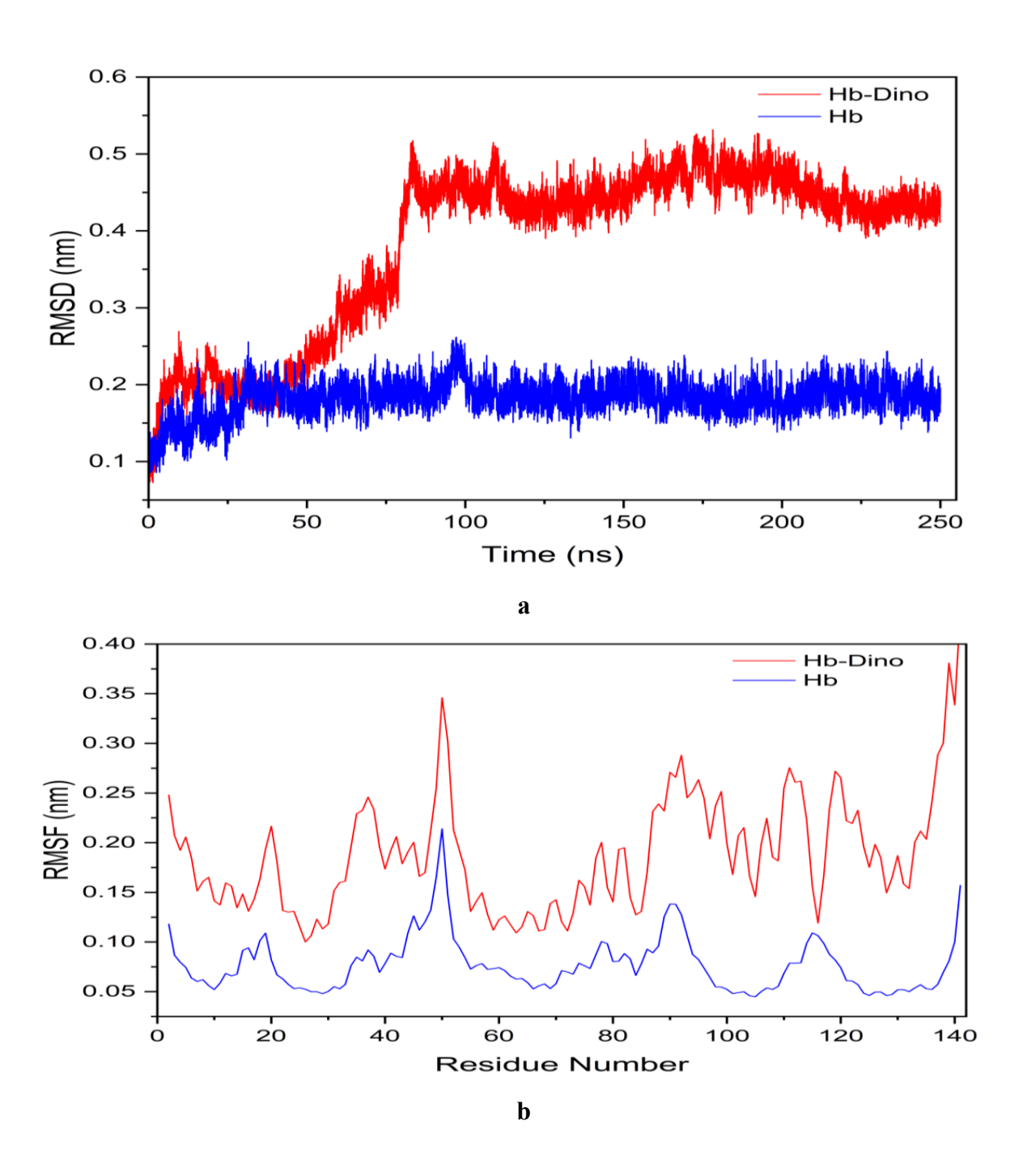


Figure 6 Two and three dimensional representation for the interaction of dinotefuran with the amino-acids of Hb

3.2.2 Molecular dynamics (MD) simulations

MD simulations of Hb with and without dinotefuran for 250 ns using Gromacs. Various trajectories are plotted to understand the stability of the Hb with and without dinotefuran. Herein, the stability of the complex is studied and compared with the protein (Hb) alone. Figure 7a represents the root mean square deviation (RMSD) plot for the Hb with and without dinotefuran. RMSD value of Hb alone attain stability in the beginning and no significant change in the RMSD values is observed. But in case of the Hb-dinotefuran, an increase in the RMSD value is observed at 50 ns and then it attains stability at 90 ns. Then, no significant increase in RMSD value is observed. Figure 7b represents the root mean square fluctuation (RMSF) for the Hb with and without dinotefuran for MD simulations performed for 250 ns. Fewer fluctuations are observed in the case of Hb than in the case of the Hb-dinotefuran complex. Further, another trajectory, that is, H-bond, is plotted for Hb-dinotefuran as in Figure 7c and a good number of hydrogen bonds are formed, indicating the stable complex (Hb-dinotefuran)^[68–70].



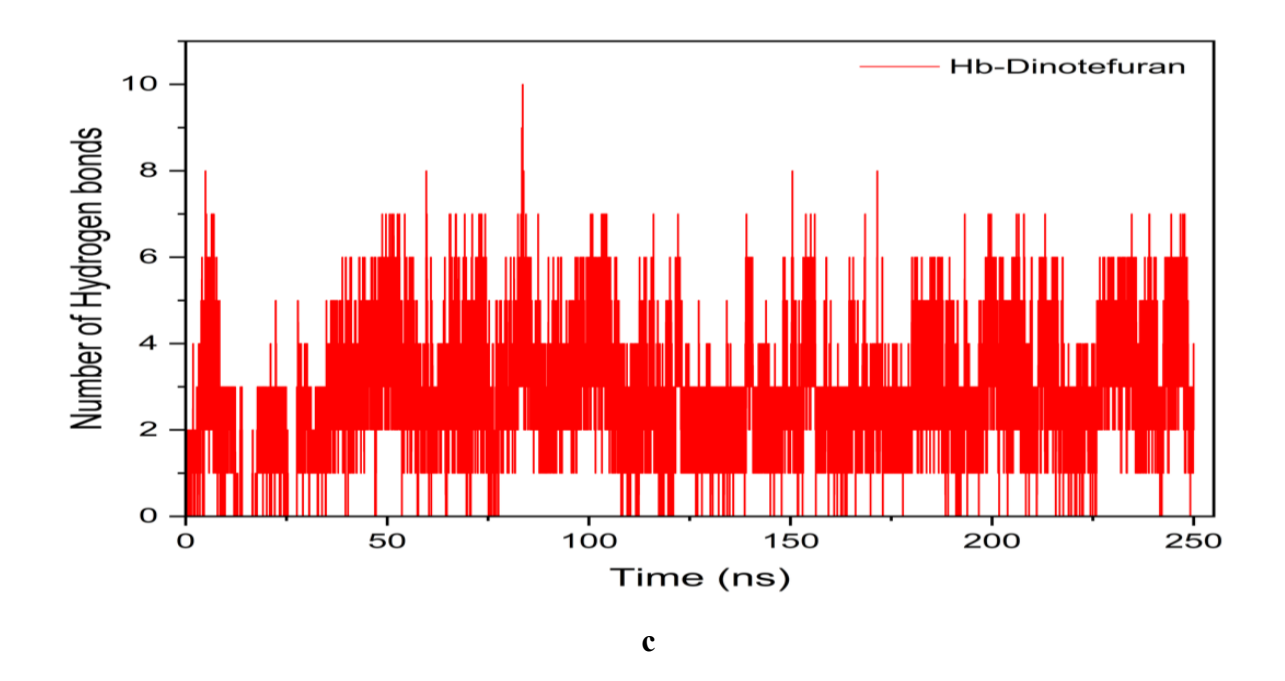


Figure 7 a) RMSD, b) RMSF and c) H-bonds trajectory for the complex (dinotefuran-Hb)

3.3.3 Molecular Mechanics Poisson-Boltzmann Surface Area (MM-PBSA) calculations

The binding free energy for the formation of the complex is determined by Molecular Mechanics Poisson-Boltzmann Surface Area (MM-PBSA). MM-PBSA is a popular method for calculating absolute binding affinities with a modest computational effort. Various thermodynamic parameter for the formation of complex is determined (Table 3). The binding free energy was calculated as -53.627 kJ/mol^[71–73].

Table 3 Different thermodynamic parameters for the formation of complex

Type of energy	Values (kJ/mol)
Van der Waal energy	-43.727
Electrostatic energy	-298.247
Polar solvation energy	296.220
SASA energy	-7.873
Binding free energy	-53.627

3.3 Electrochemical Studies

The exploration of the interplay between Dinotefuran and Hb involved leveraging the 604E electrochemical analyzer crafted by CHI Inc. This investigation utilized a three-electrode

arrangement, comprising a glassy carbon electrode (GCE) as the principal electrode, a platinum wire counter electrode, and an Ag/AgAgCl reference electrode. Operating within a potential span of -2 V to 1 V with a sensitivity setting at 1 × 10⁻³, the study aimed to discern the redox dynamics and potential interactions within the dinotefuran-Hb system. To probe the kinetics and potential-induced shifts in electrochemical behaviour, a spectrum of scan rate variations spanning 100 mV/s to 500 mV/s was meticulously explored. The concentration of dinotefuran maintained consistency at 0.1 mM, while the Hb concentration remained steady throughout. Thorough cleansing of the GCE before each measurement involved a rigorous procedure encompassing 0.3-micron alumina cleaning and subsequent sonication in deionized water, ensuring the elimination of any residual traces of prior dinotefuran or Hb adsorption. Standard solutions of dinotefuran and Hb in a pH=7.4 buffered solution (PBS) was diligently prepared, and all experiments were rigorously conducted under constant room temperature conditions.

Distinctive electrochemical behaviour of dinotefuran was observed in its cyclic voltammograms. A reductive peak at 1.48V was observed, and no other significant peak was observed. As reported in the literature the peak is due to the irreversible reduction of nitro group into amine group. Figure 8a showed the multi-scan graph of a 0.1mM solution of dinotefuran in a PBS buffer of 7.4 pH at a 500 mV/s scan rate. The peak current reduces in every successive sweep segment, signifying that molecules of dinotefuran are being adsorbed at the electrode surface area, blocking the sites for electron exchange. Thus, the electrodes were cleaned before each reading in further studies. Tafel plot analysis of dinotefuran in PBS buffer of pH 7.4 confirmed that the reduction rate of dinotefuran dominates the oxidation rate as the cathodic slope was 1.784 and anodic slope was 3.144. A lower slope indicates higher reaction kinetics. Figure 8b contains the tafel plot of 0.1mM solution of dinotefuran in PBS buffer. Interactions of dinotefuran and Haemoglobin were studied with the help of cyclic voltammetry by comparing the voltammograms of a 10mM solution of Haemoglobin and a mixture of dinotefuran and Haemoglobin (Figure 8c). A time-dependent study concluded that the reductive peak of dinotefuran was not significantly affected by the presence of Haemoglobin initially. The peak current reduced gradually over a period of time as shown in Figure 8d, indicating that the concentration of free molecules of dinotefuran in the solution was reduced. Minor shifts in the peak potential were observed, possibly due to the adsorption of Hb on the electrode surface interfering with electron transfer processes.

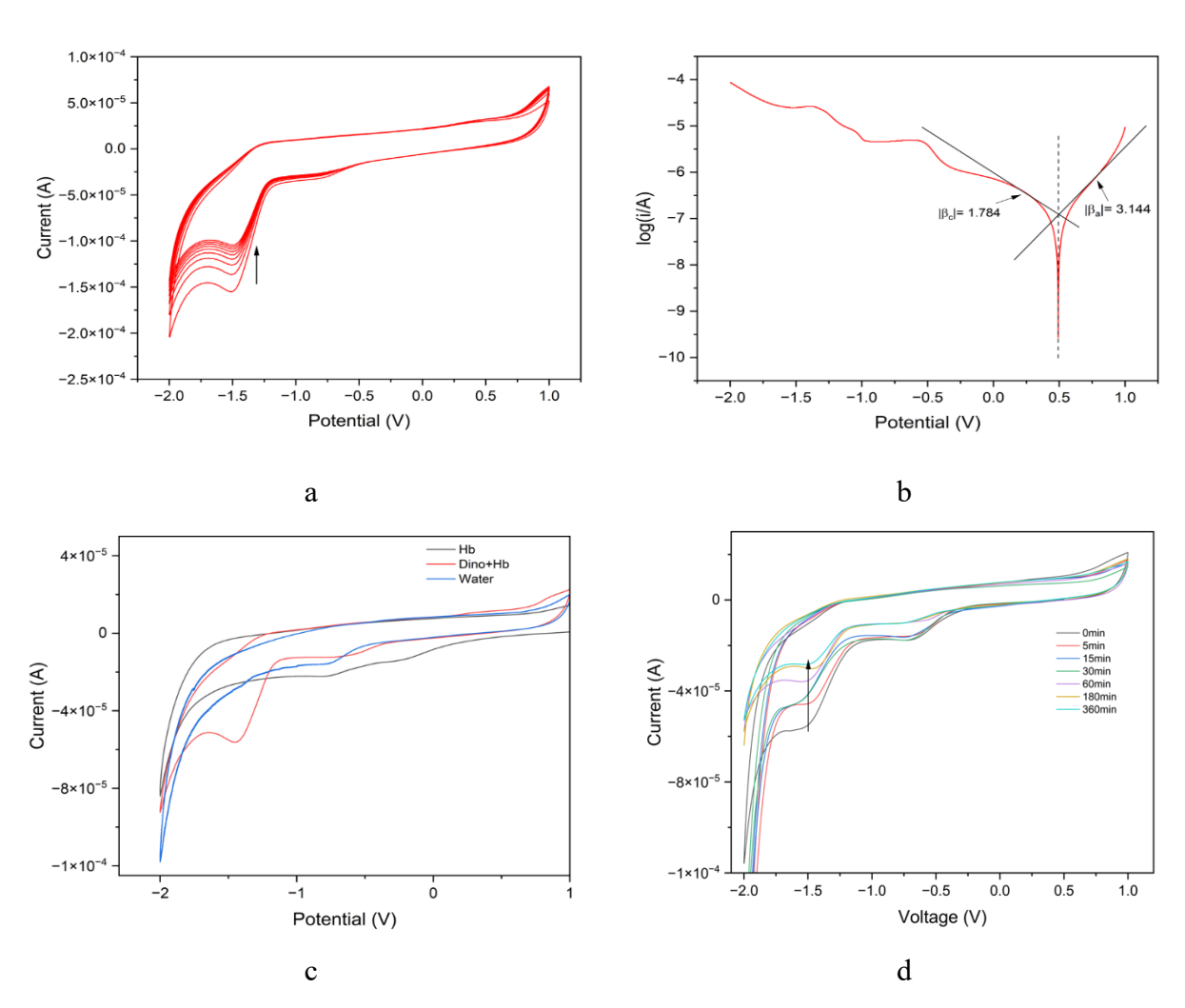


Figure 8 a) Multi-scan graph of 0.1mM dinotefuran in PBS buffer (pH=7.4), b) Tafel plot of Dinotefuran in PBS buffer (pH=7.4), c) Cyclic voltammograms of Hb solution(10μM) and Hb-Dinotefuran solution at room temperature with 1x10⁻³ sensitivity, and d) Cyclic voltammograms of Hb-Dinotefuran solution at 0, 5, 15, 30, 60, 180 and 360 minutes of mixing

The study presented a comprehensive investigation into the interactions between dinotefuran and Hemoglobin (Hb), as evidenced by various analytical techniques. UV-visible spectroscopy revealed a dose-dependent increase in Hb absorbance at 278nm with rising dinotefuran concentrations, indicating the binding of dinotefuran with Hb. Fluorescence studies established a high binding constant of $1.362 \times 10^6 \, \mathrm{M}^{-1}$, with static quenching characteristics. Molecular docking simulations elucidated a binding energy of -5.37 kcal mol⁻¹, facilitated by two hydrogen bonds and three hydrophobic interactions with Hb amino acids. Molecular dynamics (MD) simulations further supported the stability of the dinotefuran-Hb complex, with a maximal count of 10

hydrogen bonds and an average of 4-6, indicating sustained complex formation. The MMPBSA study corroborated these findings with a substantial binding energy of -53.627 kJ mol⁻¹. Additionally, electrochemical studies demonstrated the disappearance of characteristic dinotefuran peaks in the presence of Hb, further affirming their interaction. These collective results provide insight into the intricate binding dynamics between dinotefuran and Hb, offering valuable guidance for future research endeavors in related fields.

4. Conclusion

This work has examined the binding of dinotefuran to Haemoglobin by *in silico*, electrochemical, and spectroscopic techniques. UV-visible and fluorescence spectroscopy revealed the formation of a stable complex between dinotefuran and Haemoglobin. The constant temperature rises in Stern-Volmer quenching served as evidence for static quenching. A stable molecular complex formed between ofloxacin and Haemoglobin was shown via molecular docking. The binding energy for the formation of complex was found to -5.37 kcal/mol. It effectively interacts with SER, VAL, LEU and PHE at 133, 93, 101 and 98 position of the sequence. Molecular dynamics simulations provide an insight for the stability of the complex (Hb-dinotefuran) for a span of 250 ns with a binding free energy of -53.627 kJ/mol. A number of trajectories, including RMSD and RMSF, confirmed that a stable complex had developed. The peak current reduces in every successive sweep segment, signifying that molecules of dinotefuran are being adsorbed at the electrode surface area, blocking the sites for electron exchange. Tafel plot analysis of Dinotefuran in PBS buffer of pH 7.4 confirmed that the reduction rate of dinotefuran dominates the oxidation rate as the cathodic slope was 1.784 and anodic slope was 3.144. A lower slope indicates higher reaction kinetics. Interactions of dinotefuran and Hb were studied with the help of cyclic voltammetry by comparing the voltagrams of 10mM solution of Hb, and mixture of dinotefuran and Hb. A timedependent study concluded that the reductive peak of dinotefuran was not significantly affected by the presence of Hb initially. By elucidating the molecular interactions between dinotefuran and Hb, this research contributes valuable insights to the understanding of pesticide-protein interactions, laying a foundation for further exploration in related fields.

Credit authorship contribution statement

Sandeep Yadav, Shubham Sewariya, Pallavi Jain: Conceptualization, Methodology,

Investigation, Data curation, Writing – Original draft, Visualization.

Prashant Singh, Pallavi Jain, and Ramesh Chandra: Resources, review, editing, supervision.

Prashant Singh, Ramesh Chandra, and Kamlesh Kumari: Conceptualization, validation,

supervision, funding acquisition.

References

- [1] F. P. Carvalho, *Food Energy Secur* **2017**, *6*, 48–60.
- [2] M. C. R. Alavanja, M. R. Bonner, *Journal of Toxicology and Environmental Health, Part B* **2012**, *15*, 238–263.
- [3] H. de O. Gomes, J. M. C. Menezes, J. G. M. da Costa, H. D. M. Coutinho, R. N. P. Teixeira, R. F. do Nascimento, *Ecotoxicol Environ Saf* **2020**, *197*, 110627.
- [4] S. Küçükler, C. Caglayan, S. Özdemir, S. Çomaklı, F. M. Kandemir, *Metab Brain Dis* **2023**, *39*, 509–522.
- [5] M. Tudi, H. Li, H. Li, L. Wang, J. Lyu, L. Yang, S. Tong, Q. J. Yu, H. D. Ruan, A. Atabila, D. T. Phung, R. Sadler, D. Connell, *Toxics* 2022, 10, 10060335.
- [6] H. Bouwman, R. Bornman, H. van den Berg, H. Kylin, 2013.
- [7] I. C. Yadav, N. L. Devi, J. Li, G. Zhang, P. R. Shakya, *Science of the Total Environment* **2016**, *573*, 1598–1606.
- [8] S. Mostafalou, M. Abdollahi, Arch Toxicol 2017, 91, 549–599.
- [9] C. Lang, S. Tao, X. Wang, G. Zhang, J. Fu, Environmental Toxicology and Chemistry: An International Journal 2008, 27, 4–9.
- [10] G. P. Das, K. Jamil, M. F. Rahman, *Toxicol Mech Methods* **2006**, *16*, 455–459.
- [11] C. A. Damalas, I. G. Eleftherohorinos, *Int J Environ Res Public Health* **2011**, *8*, 1402–1419.
- [12] E. MacFarlane, R. Carey, T. Keegel, S. El-Zaemay, L. Fritschi, *Saf Health Work* **2013**, *4*, 136–141.
- [13] K.-H. Kim, E. Kabir, S. A. Jahan, Science of the total environment **2017**, 575, 525–535.
- [14] D. T. Phung, D. Connell, G. Miller, S. Rutherford, C. Chu, *J Agromedicine* **2013**, *18*, 293–303.
- [15] C. An, J. Cui, Q. Yu, B. Huang, N. Li, J. Jiang, Y. Shen, C. Wang, S. Zhan, X. Zhao, X. Li, C. Sun, B. Cui, C. Wang, F. Gao, Z. Zeng, H. Cui, R. Zhang, Y. Wang, *Int J Biol Macromol* 2022, 206, 633–641.
- [16] Z.-H. Jiao, S.-L. Hou, X.-M. Kang, X.-P. Yang, B. Zhao, *Anal Chem* **2021**, *93*, 6599–6603.
- [17] P. Jeschke, R. Nauen, M. Schindler, A. Elbert, *J Agric Food Chem* **2011**, *59*, 2897–2908.
- [18] M. F. Abdel-Ghany, L. A. Hussein, N. F. El Azab, *Talanta* **2017**, *164*, 518–528.
- [19] H. Li, L. Wang, Tetrahedron 2018, 74, 336–340.

- [20] K. Kobashi, T. Harada, Y. Adachi, M. Mori, M. Ihara, D. Hayasaka, *Ecotoxicol Environ Saf* **2017**, *138*, 122–129.
- [21] B. Yu, Z. Chen, X. Lu, Y. Huang, Y. Zhou, Q. Zhang, D. Wang, J. Li, *Science of the Total Environment* **2020**, *725*, 138328.
- [22] A. Cartereau, J.-N. Houchat, S. Mannai, M. Varloud, H. Karembé, J. Graton, J.-Y. Le Questel, S. H. Thany, *Neurotoxicology* **2018**, *67*, 206–214.
- [23] D. A. Gell, Blood Cells Mol Dis 2018, 70, 13–42.
- [24] G. Sabbioni, H. G. Neumann, *Carcinogenesis* **1990**, *11*, 111–115.
- [25] A. K. Sharma, K. Gaur, R. K. Tiwari, M. S. Gaur, *J Biomed Res* **2011**, *25*, 335–347.
- [26] D. S. Buss, A. Callaghan, *Pestic Biochem Physiol* **2008**, *90*, 141–153.
- [27] A. Arif, Md. A. Hashmi, S. Salam, H. Younus, R. Mahmood, *J Biomol Struct Dyn* **2023**, 41, 6591–6602.
- [28] V. Bhat, P. Nayak, S. Bakkannavar, P. Udupa, *F1000Res* **2023**, *12*, 478.
- [29] M. Emadi, P. Maghami, K. Khorsandi, R. Hosseinzadeh, *J Biochem Mol Toxicol* **2019**, *33*, e22325.
- [30] A. Doroudian, R. Hosseinzadeh, P. Maghami, K. Khorsandi, *J Biomol Struct Dyn* **2022**, 40, 7786–7795.
- [31] K. Kumari, M. B. Singh, N. Tomar, A. Kumar, V. Kumar, K. L. Dabodhia, P. Singh, *J Mol Struct* **2023**, *1291*, 136043.
- [32] M. Abrar Siddiquee, J. Saraswat, M. ud din Parray, P. Singh, S. Bargujar, R. Patel, Spectrochim Acta A Mol Biomol Spectrosc 2023, 285, 121803.
- [33] W. Bae, T. Y. Yoon, C. Jeong, *PLoS One* **2021**, *16*, e0247326.
- [34] K. Azeem, M. Ahmed, T. Mohammad, A. Uddin, A. Shamsi, M. I. Hassan, S. Singh, R. Patel, M. Abid, *J Biomol Struct Dyn* **2022**, 2107077.
- [35] K. R. Cousins, J Am Chem Soc 2005, 127, 4115–4116.
- [36] G. M. Morris, H. Ruth, W. Lindstrom, M. F. Sanner, R. K. Belew, D. S. Goodsell, A. J. Olson, *J Comput Chem* **2009**, *30*, 2785.
- [37] D. Van Der Spoel, E. Lindahl, B. Hess, G. Groenhof, A. E. Mark, H. J. C. Berendsen, *J Comput Chem* **2005**, *26*, 1701–1718.
- [38] K. K. Hussain, J. M. Moon, D. S. Park, Y. B. Shim, *Electroanalysis* **2017**, *29*, 2190–2199.
- [39] A. Salimi, E. Sharifi, A. Noorbakhsh, S. Soltanian, Electrochem commun 2006, 8, 1499– 1508.

- [40] S. V. Sokolov, L. Sepunaru, R. G. Compton, Appl Mater Today 2017, 7, 82–90.
- [41] H. H. Dimer, W. L. Nichols, B. H. Zimm, L. F. Ten Eyck, *J Mol. Bio.* **1997**, *270*, 598-615.
- [42] S. Sewariya, H. Sehrawat, N. Mishra, M. B. Singh, P. Singh, S. Kukreti, R. Chandra, *Int J Biol Macromol* **2023**, *247*, 125791.
- [43] M. Kirici, M. Kirici, Y. Demir, S. Beydemir, M. Atamanalp, *Appl. Ecol. Environ. Res.* **2016**, *14*, 253–264.
- [44] Z. Alım, D. Kılıç, Y. Demir, Arch Physiol Biochem 2019, 125, 387–395.
- [45] J. H. Shi, Y. Y. Lou, K. L. Zhou, D. Q. Pan, J Photochem Photobiol B 2018, 180, 125–133.
- [46] Q. Wang, C. R. Huang, M. Jiang, Y. Y. Zhu, J. Wang, J. Chen, J. H. Shi, *Spectrochim Acta A Mol Biomol Spectrosc* **2016**, *156*, 155–163.
- [47] J. H. Shi, Q. Wang, D. Q. Pan, T. T. Liu, M. Jiang, J Biomol Struct Dyn 2017, 35, 1529– 1546.
- [48] N. Kritika, M. Pant, M. Yadav, A. K. Verma, A. K. Mahapatro, I. Roy, *J Mater Chem B* **2023**, *11*, 4785-4798.
- [49] B. L. Wang, D. Q. Pan, K. L. Zhou, Y. Y. Lou, J. H. Shi, Spectrochim Acta A Mol Biomol Spectrosc 2019, 212, 15–24.
- [50] B. L. Wang, S. B. Kou, Z. Y. Lin, J. H. Shi, Y. X. Liu, *Int J Biol Macromol* **2020**, *157*, 340–349.
- [51] B. L. Wang, S. B. Kou, Z. Y. Lin, J. H. Shi, *Spectrochim Acta A Mol Biomol Spectrosc* **2020**, *232*, 118160.
- [52] F. F. Tian, J. H. Li, F. L. Jiang, X. Le Han, C. Xiang, Y. S. Ge, L. L. Li, Y. Liu, *RSC Adv* **2011**, *2*, 501–513.
- [53] S. Hazra, G. Suresh Kumar, Journal of Physical Chemistry B 2014, 118, 3771–3784.
- [54] B. Alpert, D. M. Jameson, G. Weber, *Photochem Photobiol* **1980**, *31*, 1–4.
- [55] B. L. Wang, D. Q. Pan, K. L. Zhou, Y. Y. Lou, J. H. Shi, Spectrochim Acta A Mol Biomol Spectrosc 2019, 212, 15–24.
- [56] Y. F. Zhang, K. L. Zhou, Y. Y. Lou, D. Q. Pan, J. H. Shi, J Biomol Struct Dyn 2017, 35, 3605–3614.
- [57] Q. Wang, C. R. Huang, M. Jiang, Y. Y. Zhu, J. Wang, J. Chen, J. H. Shi, *Spectrochim Acta A Mol Biomol Spectrosc* **2016**, *156*, 155–163.
- [58] S. B. Corchnoy, T. E. Swartz, J. W. Lewis, I. Szundi, W. R. Briggs, R. A. Bogomolni, *Journal of Biological Chemistry* **2003**, *278*, 724–731.

- [59] B. OXYGEN heimer, J. R. Lakowicz, G. Weber, *QUENCHING OF FLUORESCENCE Quenching of Fluorescence by Oxygen. A Probe for Structural Fluctuations in Macromoleculest*, Weber, G, **1966**.
- [60] A. Manna, S. Chakravorti, *Mol Biosyst* **2013**, *9*, 246–257.
- [61] J. Q. Tong, F. F. Tian, Q. Li, L. Li, C. Xiang, Y. Liu, J. Dai, F. L. Jiang, *Photochemical and Photobiological Sciences* **2012**, *11*, 1868–1879.
- [62] F. F. Tian, J. H. Li, F. L. Jiang, X. Le Han, C. Xiang, Y. S. Ge, L. L. Li, Y. Liu, *RSC Adv* **2012**, *2*, 501–513.
- [63] F. F. Tian, F. L. Jiang, X. Le Han, C. Xiang, Y. S. Ge, J. H. Li, Y. Zhang, R. Li, X. L. Ding, Y. Liu, *Journal of Physical Chemistry B* **2010**, *114*, 14842–14853.
- [64] C. References Bjurulf, I. Wadsó, V. W. Dimmling, E. Lange, L. Grenthe, H. Ots, O. Ginstrup, W. Pfeil, P. L. Privalov, J. M. Sturtevant, P. A. Lyons, *Thermodynamics of Protein Association Reactions: Forces Contributing to Stability1*, **1972**.
- [65] R. Zengin, Y. Gök, Y. Demir, B. Şen, T. Taskin-Tok, A. Aktaş, Ö. Demirci, İ. Gülçin, M. Aygün, *J Fluor Chem* **2023**, *267*, 110094.
- [66] Y. Demir, C. Türkeş, M. S. Çavuş, M. Erdoğan, H. Muğlu, H. Yakan, Ş. Beydemir, *Arch Pharm (Weinheim)* **2023**, *356*, 2200554.
- [67] M. Yiğit, Y. Demir, D. Barut Celepci, T. Taskin-Tok, A. Arınç, B. Yiğit, M. Aygün, İ. Özdemir, İ. Gülçin, *Arch Pharm (Weinheim)* **2022**, *355*, 2200348.
- [68] Mohd. Aslam, G. Pandey, N. Deshwal, A. Kumar, K. Kumari, I. Bahadur, P. Singh, F. Mohammad, A. Abdullah Soleiman, *J Mol Liq* **2024**, *397*, 124070.
- [69] C. J. Morris, D. Della Corte, *Modern Physics Letters B* **2021**, *35*, 2130002.
- [70] R. Shukla, T. Tripathi, Computer-Aided Drug Design 2020, 133–161.
- [71] Y. X. Zhu, Y. J. Sheng, Y. Q. Ma, H. M. Ding, *Journal of Physical Chemistry B* **2022**, *126*, 1700–1708.
- [72] S. Genheden, U. Ryde, Expert Opin Drug Discov 2015, 10, 449–461.
- [73] K. Huang, S. Luo, Y. Cong, S. Zhong, J. Z. H. Zhang, L. Duan, *Nanoscale* **2020**, *12*, 10737–10750.